# INTERNATIONAL SOCIETY FOR SOIL MECHANICS AND GEOTECHNICAL ENGINEERING

# Air permeability measurements in low porosity clayey rocks

*Jubert* Pineda[1#], *Hoang Viet* Nguyen[2], *Enrique* Romero[3], *Daichao* Sheng[4] and *Antonio* Gens[3]

[1]*The University of Newcastle, School of Engineering, Callaghan Campus, Newcastle NSW, Australia*
[2]*Hanoi University of Civil Engineering, Hanoi, Vietnam (formerly at The University of Newcastle, Australia)*
[3]*Technical University of Catalonia, UPC, Barcelona, Spain*
[4]*University of Technology Sydney, UTS, Sydney, Australia*
[#]*Corresponding author: Jubert.pineda@newcastle.edu.au*

## ABSTRACT

The paper describes the development of a high-pressure isotropic cell for studying the environmental degradation of low porosity clayey rocks. Air permeability measurements are used in this device as a tool to evaluate rock degradation in unsaturated rock specimens caused by mechanical, hydraulic and chemical paths. A modified equation, based on the air pressure decay method proposed by Yoshimi and Osterberg (1963), is presented. The proposed method is applied to an Australian clayey shale. Estimated values of air permeability are compared against those calculated using the original method which, in the case of low porosity rocks, seems to provide unrealistic values when the air pressure in the vessel decays beyond 50%.

**Keywords:** air permeability; clayey rock; rock degradation.

## 1. Introduction

The hydraulic properties of clayey rocks play a key role on the behaviour of slopes, foundations and excavations. However, its estimation either in situ or in the laboratory is not trivial. One major reason, at least for the characterization of the hydraulic properties in the laboratory, is the irreversible change in rock structure that may take place when clayey rocks are exposed to liquid water at low stress levels. In those cases, an interesting alternative is the estimation of the air permeability, considering the minor effect of air on rock structure (e.g. Harrington and Horseman, 1999; Pineda et al., 2014a; Nguyen, 2020). This testing technique is becoming more popular due to the need for proper understanding of gas transport processes in clayey formations as part of energy-related geotechnical problems (e.g. Olivella and Alonso, 2008; Romero et al., 2012; Cevatoglu et al., 2015; Nguyen et al., 2021; Gonzalez-Blanco and Romero, 2023).

This paper presents the main features of a novel high-pressure isotropic cell designed to study the hydraulic and mechanical behaviour of low permeability clayey rocks. The paper reports air permeability tests carried out on shale specimens previously exposed to relative humidity (RH) cycles. The performance of two air permeability models is discussed. The proposal by Yoshimi and Osterberg (1963) is first presented and some discrepancies between the experimental results and the assumptions in the air permeability model are highlighted. The derivation of a modified expression aimed at improving the permeability estimations is also presented. The comparison of these two methods indicates that the new proposal seems to overcome the issue of the original method in which the nonlinearity of the air pressure decay curve is not properly captured when the air pressure in the vessel decays beyond 40-50%. Nevertheless, both models show very similar results when only the first part of the test results are used (air pressure decay in the vessel < 40 %).

## 2. Material

The rock tested is Ashfield shale, a low porosity sedimentary (Triasic) rock from the Sydney Basin (Herbert, 1979) mainly composed of Kaolinite (31.1%), Quartz (27.7%), Illite (21%) and Muscovite (18%). The structure of the rock is highly laminated which causes large degree of anisotropy in its mechanical properties (e.g. Ghafoori, 1995; William and Airey, 2004; Nguyen, 2020; Ou, 2021). Tested specimens had a porosity between 0.05 – 0.13, dry density around 2.15 – 2.7 Mg/m$^3$ and density of solid particles of 2.68 Mg/m$^3$. Figure 1 shows a picture of the rock cores and samples tested in this study. Specimens for laboratory testing were obtained from rock cores retrieved between 20.5 – 22 m depth. A mechanical lathe was used to trim cylindrical specimens of 38 mm in diameter and 38 mm in height.

## 3. Equipment and procedures

Laboratory tests were carried out in a novel high-pressure isotropic apparatus designed at the University of Newcastle (UoN) to study the hydro-mechanical behaviour of clayey rocks (see Figure 2) (Nguyen, 2020). Most features of this device resemble those of the high-pressure triaxial apparatus developed by Pineda et al. (2014a). Auxiliary systems allow the application of

wetting-drying cycles via the vapour transfer technique (Blatz et al., 2008), the evaluation of the unsaturated rock permeability via gas pulse tests as well as the estimation of the small-strain shear stiffness using bender elements transducers (Arroyo et al., 2010). A modified version of this device (Ou, 2021) also allows the control/monitoring of the pore fluid chemistry in saturated tests.
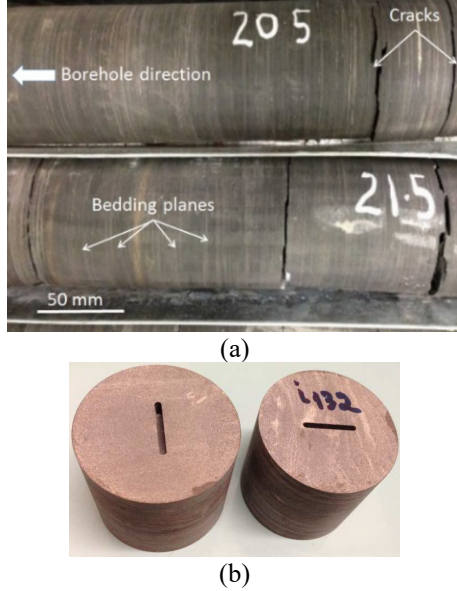


(a)



(b)

**Figure 1.** Ashfield shale. (a) rock cores. (b) samples tested (slots are used for bender elements testing)

The isotropic cell has an inner diameter of 150 mm that enables the use of internal instrumentation on cylindrical specimens of two different diameters (38 mm or 50 mm). The configuration of the internal instrumentation is shown in Figure 2(b). Axial displacements are measured locally using a pressure compensated LVDT (RDP model D6/02500U/239) whereas a pressure compensated radial extensometer (Epsilon Technology Corp.) is used to measure radial displacements. Radial stress is controlled through a 32 MPa capacity volume/pressure controller (GDS Instruments, UK). Silicone oil is used as cell fluid to avoid interferences with the internal instrumentation.

Gas pulse tests are used to evaluate the air permeability of unsaturated specimens. The test is performed using a pressurized tank of known volume V and at an initial pressure $p_0$ (upstream vessel) that is connected to the bottom cap, whereas the top cap is maintained under atmospheric conditions. The time evolution of the absolute air pressure decay $p_t$ inside the tank is recorded, which can be used to estimate the air permeability. The tank is made of stainless steel and has 50 mm in diameter and 350 mm in height. The interpretation of the test results is presented in following sections.

## 4. Experimental program

Results from three tests, performed on specimens previously subjected to different number of wetting-drying cycles under unstressed conditions, are presented in this paper. Hence, these specimens represent different rock degradation states caused by environmental actions. Table 1 summarizes the initial state of rock specimens

prior to air permeability testing. All specimens were equilibrated under a relative humidity of RH ≈ 50% before setting up in the isotropic cell.

Samples were initially loaded isotropically to mean stress of p=1MPa. After completing the first air permeability test, each sample was subsequently loaded to a mean stress of p=2 MPa and the air permeability was again estimated. A stress rate of 1 kPa/min was adopted during isotropic loading paths. An equalization time between 12-24 h was allowed to all specimens after achieving the target mean stresses. In the air permeability tests, an initial gas pressure of $p_0$ = 800 kPa was adopted and the pressure decay inside the air tank was then recorded. To minimize fluctuations in air pressure due to thermal variations, the air tank was immersed in a water bath.
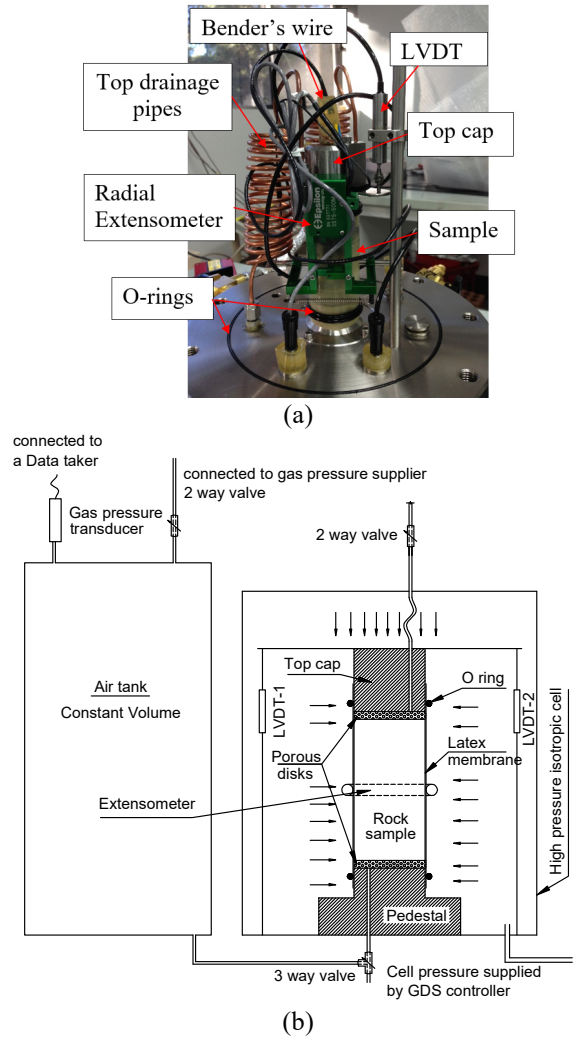


(a)



(b)

**Figure 2.** Ashfield shale cores tested in this study.

**Table 1.** State of specimens prior air permeability tests

| ID | # RH cycles | w/c (%) | $e_0$ (-) | $\varepsilon_{v\,(p=1MPa)}$ (%) | $\varepsilon_{v\,(p=2MPa)}$ (%) |
|---|---|---|---|---|---|
| i25 | 0 | 1.21 | 0.097 | 0.15 | 0.25 |
| i18C3 | 3 | 1.12 | 0.108 | 0.20 | 0.33 |
| i20 | 4 | 1.07 | 0.119 | 0.35 | 0.53 |

w/c= water content; $e_0$= void ratio after RH cycling

## 5. Test results

Table 1 reports the void ratios of rock specimens before testing in the high-pressure isotropic cell. Differences in void ratio between specimens are attributed to the application of RH cycles prior to air permeability testing which has caused rock degradation. Rock degradation is also reflected in terms of the increase in volumetric strain measured at the end of each loading step (see Table 1). This response is similar to the behaviour reported by Pineda et al. (2014a,b) for Lilla claystone from Spain.

Figure 3 shows the air pressure decay curves, $p_t/p_0$ vs. time, recorded during the application of the gas pulse at p = 1MPa and p = 2MPa. For the intact specimen (i25), the gas pressure reduces by less than 12% after 8.5h (30,000 s) of testing irrespective of the mean effective stress. However, specimens previously subjected to RH cycles show a much larger reduction during the same period. This behaviour is also controlled by the number of RH cycles applied prior to air permeability testing. It indicates an enhancement of preferential pathways for gas flow attributed here to the RH history of each sample. It may be noted that air pressure decay curves are largely non-linear, particularly after the first 9 h of testing. This behavioiur and its consequences on the estimated permeability is discussed in following sections.
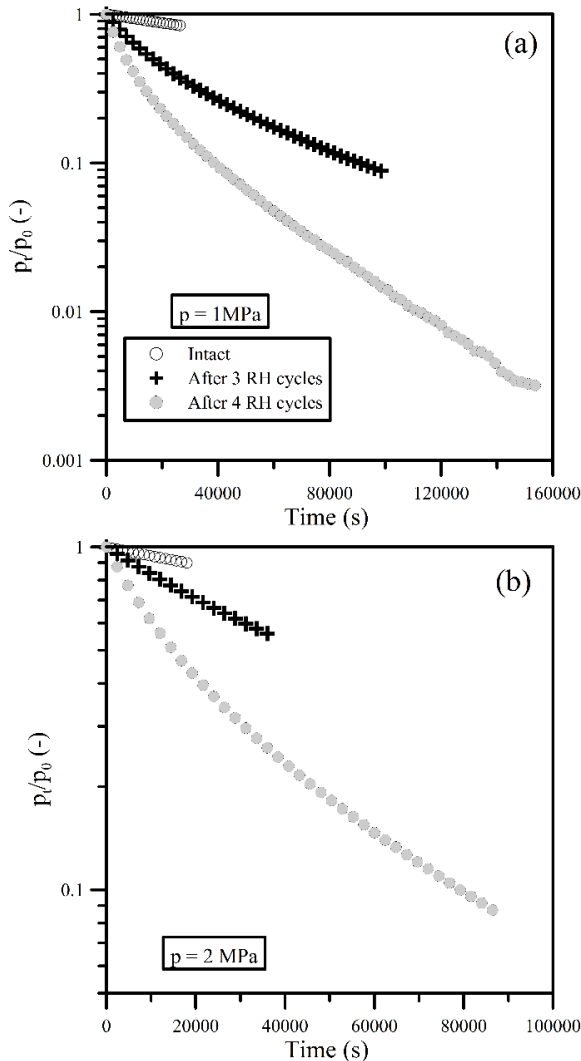


**Figure 3.** Normalized pressure decay curves

## 6. Estimation of air permeability based on Yoshimi and Osterberg (1963)

Yoshimi and Osterberg (1963) derived the following equation for the estimation of the air permeability in unsaturated soils based on the gas pressure decay method:

$$k_a(m^2) = \frac{2.3Vh\mu_a}{A\left(p_a+\frac{p_0}{4}\right)} \frac{-log_{10}\left(\frac{p_t}{p_0}\right)}{t} \qquad (1)$$

where V is the volume of the air tank [$m^3$], A is the cross section area of the specimen [$m^2$], h is the specimen height [m], $\mu_a$ is the dynamic viscosity of the air [$N.s/m^2$], $p_a$ is the atmospheric pressure [kPa], $p_0$ is the air pressure inside the tank at the beginning of the test [kPa], $p_t$ is the pressure in the air tank at a given time t [kPa]. The term $-log_{10}(p_t/p_0)/t$ refers to the slope of the air pressure decay curve, assumed to be constant during the test. In other words, the model assumes an exponential decay of air pressure with time.

Equation (1) is based on three main assumptions. First, the flow of air through the soil is viscous and free from slippage and the soil hydraulic conductivity may be described using Darcy's law:

$$v_{zt} = -\frac{k_a}{\mu_a}\frac{\partial u_{zt}}{\partial z} \qquad (2)$$

where $v_{zt}$ is the volume flux of air per unit area of sample at time t and distance z (from the bottom of the specimen), $u_{zt}$ is the gage pressure of air at time t and distance z, $k_a$ is the coefficient of permeability. Second, the dissipation of air pressure within the tank takes place under isothermal conditions. By applying the condition of continuity of mass of air to the system (i.e. soil sample + tank of air), Yoshimi and Osterberg (1963) derived the following equation:

$$\frac{dp_t}{dt} = -\frac{Ak_a}{V\mu_a}\left(p_a + \frac{p_t}{2}\right)\frac{p_t}{h} \qquad (3)$$

Equation (3) suggest that the time rate of change of the air pressure in the tank is nearly proportional to the average pressure gradient $p_t/h$. Last but not least, Yoshimi and Osterberg limited the initial air pressure inside the tank to values lower than the atmospheric pressure (i.e. $p_0 < p_a$):

$$p_a + \frac{p_t}{2} \cong p_a + \frac{p_0}{4} \qquad (4)$$

This restriction was included to minimize any flow of liquid water from the soil to the atmosphere (drying) during the application of the air pressure gradient. The combination of Equations (3) and (4) led to the derivation of Equation (1) which provides reliable estimations in soils with an open fabric. Nevertheless, the application of low pressure gradients is not experimentally advantageous for geomaterials with very low porosity so that values of $p_0>p_a$ are recommended. Romero et al.

(2005) proposed a modification of Equation (1) by replacing $p_0$ in the denominator with the average pressure inside the tank $\bar{p}_t$, which leads to:

$$k_a = \frac{Vh\mu_a}{A\left(p_a+\frac{p_t}{2}\right)}\frac{-ln\left(\frac{p_t}{p_0}\right)}{t} \qquad (5)$$

Figure 4 shows the normalized pressure decay curves for Ashfield shale specimens. Experimental results are fitted using Equation (5). Good agreement ($R^2 > 0.999$) is observed for the first part of the test when the air pressure decay is just 10%. Further reduction in the normalized air pressure shows a nonlinear relationship with time, a feature that cannot be captured by the linear model assumed in Equation (5). Figure 4 suggests that the error introduced by this nonlinearity on the estimated air permeability seems to depend on the degradation state but also the confining level applied to the rock during the test. This aspect is discussed in following sections.
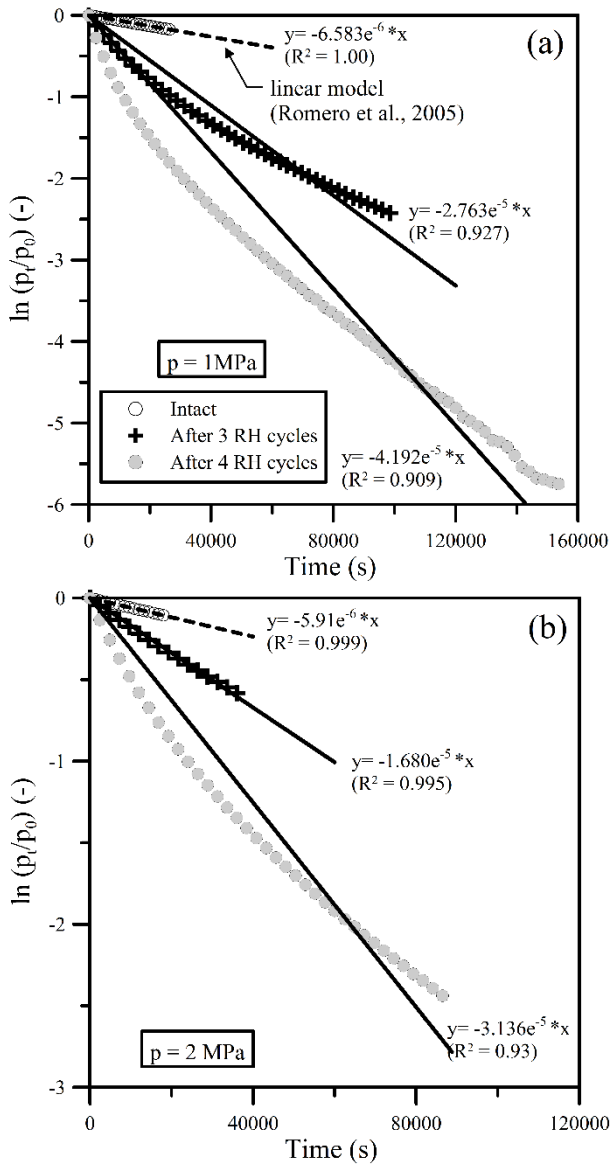


**Figure 4.** Air pressure decay curves plotted according to Equation (5)

# 7. A modified equation for the estimation of air permeability

A modified expression for the estimation of the air permeability is presented here. The new equation is based on the original work by Yoshimi and Osterberg (1963) but allowing for values of $p_0$ greater than $p_a$. To do so, Equation (3) is re-arranged and integrated for $0 < t <$ end of the test (Nguyen, 2020):

$$\int_0^t \frac{dp_t}{\left(p_a+\frac{p_t}{2}\right)p_t} = \int_0^t -\frac{A}{Vh}\cdot\frac{k_a}{\mu_a}\cdot dt \qquad (6)$$

The integration of the right-side leads to:

$$\int_0^t -\frac{A}{Vh}\frac{K_a}{\mu_a}dt = -\frac{A}{Vh}\frac{K_a}{\mu_a}t \qquad (7)$$

On the other hand, the integration of the left-side results in (see the full derivation in Nguyen, 2020):

$$\int_0^t \frac{dp_t}{\left(p_a+\frac{p_t}{2}\right)p_t}$$
$$= \frac{1}{p_a}\cdot ln\left[\frac{p_t(2p_a+p_0)}{p_0(2p_a+p_t)}\right] \qquad (8)$$

After replacing Equations (7) and (8) into Equation (6), the following expression is obtained0:

$$k_a = \frac{Vh\mu_a}{A}\cdot\frac{1}{p_a}\cdot\frac{-ln\left[\frac{p_t(2p_a+p_0)}{p_0(2p_a+p_t)}\right]}{t} \qquad (9)$$

Figure 5 shows the air pressure decay curves expressed as $ln[p_t(2p_a+p_0)/p_0(2p_a+p_t)]$ vs t. Solid and dashed lines in this figure refer to fitting curves which display regression coefficients of $R^2>0.999$. The proposed equation shows a better fitting of the experimental data which (a priori) improves the reliability of the estimated permeability for Ashfield shale specimens.

# 8. Discussion

Figure 6 compares the performance of Equation (5) and Equation (9) used for the estimation of the air permeability in Ashfield shale specimens. The results obtained for specimen i20 (after 4 RH cycles) under p = 1 MPa are used here as an example. Values of the coefficient of regression $R^2$, $ln(p_t/p_0)$, $ln[p_t(2p_a+p_0)/p_0(2p_a+p_t)]$, $\bar{p}_t$, and $k_a$ are plotted in this figure as a function of the normalized air pressure $p_t/p_0$ inside the vessel. Similar values of $R^2$ are obtained when the pressure decay inside the vessel is less than 30%. Beyond that, the $R^2$ obtained with the model by Romero et al. (2005) reduces with $p_t/p_0$, i.e. as more data is used in the analysis, to a minimum value around 0.89. On the

other hand, the proposal presented in this paper (empty circles) shows values of $R^2 > 0.999$ irrespective of the normalized pressure $p_t/p_0$. The logarithmic term in Equation (5) reduces progressively whereas the term in Equation (9) remains constant with decreasing in $p_t/p_0$. Differences in the estimated air permeability are only noticeable for $p_t/p_0 < 0.5$. Whereas the air permeability estimated via Equation (9) remains constant at around $6 \times 10^{-17}\,\text{m}^2$, it reduces to $3 \times 10^{-17}\,\text{m}^2$ if all the experimental results are used in Equation (5).

magnitude and is only relevant when the pressure decay inside the tank is higher than 40-50%.

Irrespective of the model adopted, Figure 7 shows a large variation in $k_a$ for a change in rock porosity of less than 3%. According to Nguyen (2020), this is the result of micro fissuring which creates preferential pathways for fluid flow. Such a behaviour is largely irreversible, for engineering purposes, as the permeability of the intact rock is not recovered after the application of large confining stresses.
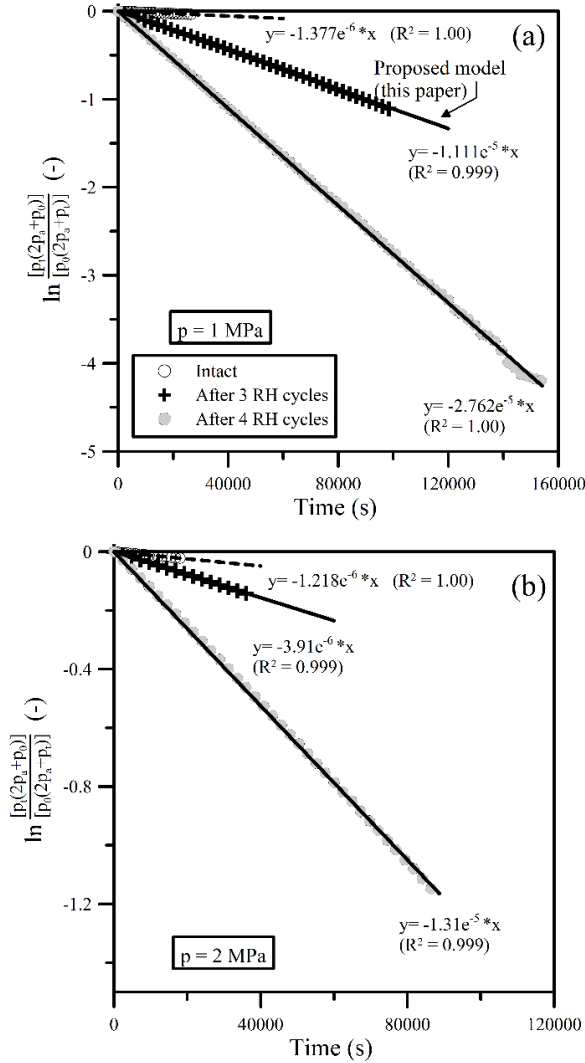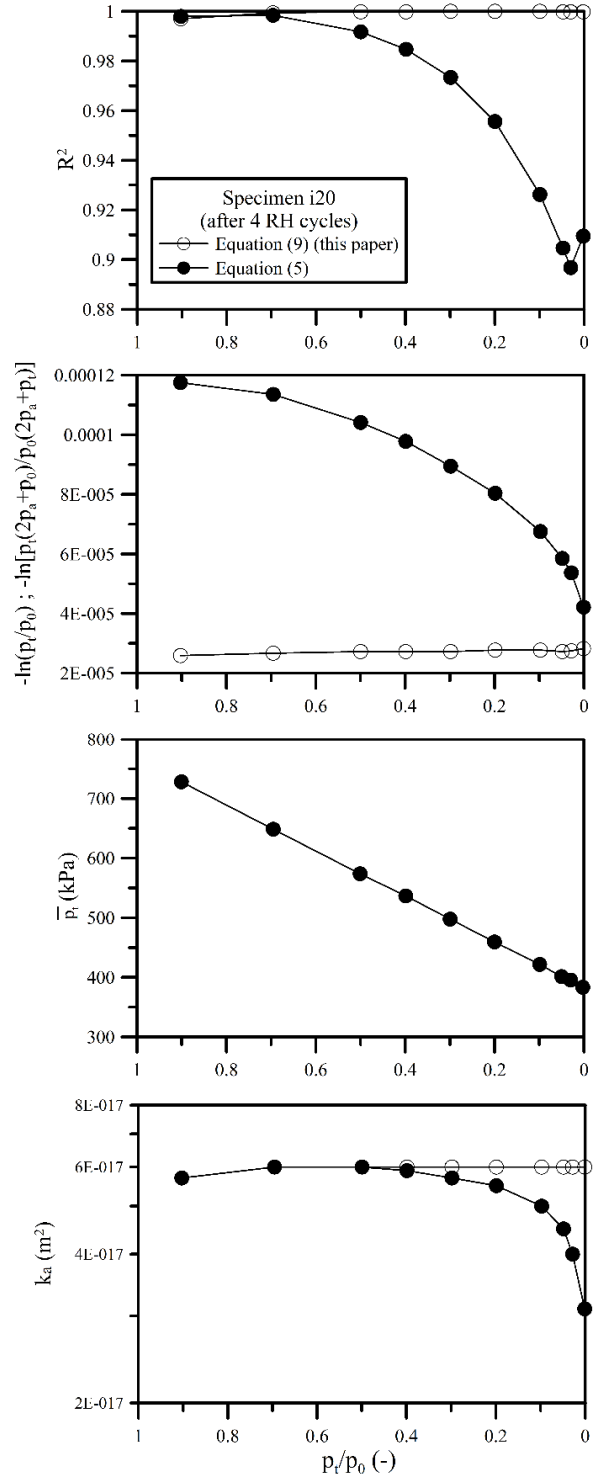


**Figure 5.** Air pressure decay curves plotted according to Equation (9)

Figure 7 shows the variation of the air permeability with rock porosity for Ashfield shale specimens. Values obtained using Equation (5) (open circles) and Equation (9) (filled circles) are presented in this figure. It may be noted that the full data set was used in the estimation of $k_a$ presented in Figure 7. Air permeability for intact rock ranges around $10^{-18}\,\text{m}^2$. The application of RH cycles causes an increase in air permeability of more than one order of magnitude. Equation (9) proposed in this paper predicts higher values of $k_a$ compared to Equation (5). Taking into account the better fitting observed in Figure 5, those estimates may be considered more reliable. Nevertheless, the maximum difference in $k_a$ obtained from these two methods is less than one order of



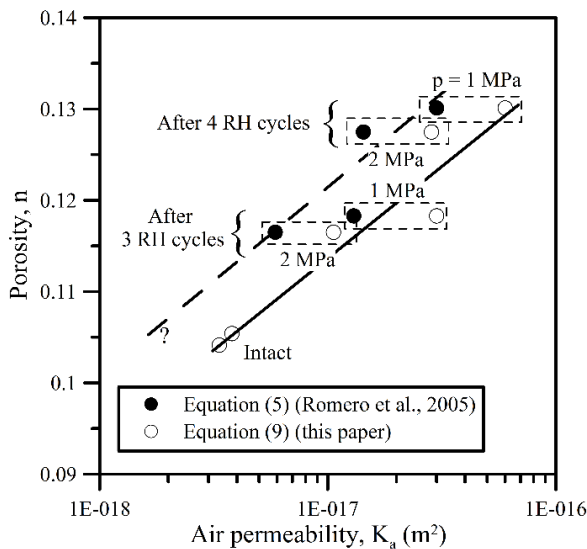**Figure 6.** Performance of both air permeability models (results for sample i20 at p = 1MPa)

**Figure 7.** Variation of air permeability with rock porosity

## 9. Final remarks

The main features of a new high-pressure isotropic cell for hard soils and soft rocks were presented in this paper. Air permeability measurements were performed on specimens of Ashfield shale previously subjected to different degradation states via RH cycling. A modified expression has been proposed in this paper for the estimation of the air permeability in low porosity rocks. Whereas the new expression provides better fitting of the experimental data which in turn gives more reliable air permeability estimates, similar results may be obtained with the original expression (Equation 5) if just the initial part of the air pressure decay curve is used in the analysis. From a practical perspective, the results presented in this paper indicate that reliable estimates of air permeability require no more than 40% air pressure decay inside the vessel which, in turn, may reduce the actual testing time in low porosity rocks.

## Acknowledgements

## References

Arroyo, M., Pineda, J.A. and Romero, E. 2010. "Shear wave measurements using bender elements in argillaceous rocks." Geotechnical Testing Journal, 33(6), 1-10. 10.1520/GTJ102872

Blatz, J., Cui, Y-J. and Oldecop, L. 2008. "Vapour equilibrium and osmotic technique for suction control." Geotechnical and Geological Engineering, 26, 661-673. 10.1007/978-1-4020-8819-3_5

Cevatoglu, M., Bull, J. M., Vardy, M. E., Gernon, T. M.,Wright, I. C. and Long, D. 2015. "Gas migration pathways, controlling mechanisms and changes in sediment acoustic properties observed in a controlled sub-seabed CO2releaseexperiment." Int. J. Greenh. Gas Control 38, 26–43, https://doi.org/10.1016/j.ijggc.2015.03.005

Ghafoori, M. 1995. "Engineering behaviour of Ashfield shale." PhD Thesis, University of Sydney.

Herbert, C. 1979. "The geology and resource potential of the Wianamatta Group." Bulletin of Geological Survey of Engineering Geology and the Environment, 25.

Gonzalez-Blanco, L. and Romero, E. 2023. "A multi-scale insight into gas transport in a deep Cenozoic clay." Geotechnique (in print), https://doi.org/10.1680/jgeot.21.00208 Harrington, J. F. and Horseman, S. T. 1999. "Gas transport properties of clays and mudrocks." Geological Society London, Special Publication 158, No.1, 107–124, https://doi.org/10.1144/GSL.SP.1999.158.01.09

Nguyen, V.H. 2020. "Environmental effects on the hydro-mechanical behaviour of Ashfield shale." PhD Thesis, the University of Newcastle Australia.

Nguyen, V.H., Pineda, J.A., Romero, E. and Sheng D. 2021. "Influence of soil microstructure on air permeability in compacted clay." Geotechnique, 71(5), 373-391. https://doi.org/10.1680/jgeot.18.P.186

Olivella, S. and Alonso, E. E. 2008. "Gas flow through clay barriers." Géotechnique, 58(3), 157–176, https://doi.org/10.1680/geot.2008.58.3.157

Ou, K. 2021, "Experimental and theoretical investigation on the chemo-hydro-mechanical behaviour of hard soils-soft rocks." PhD Thesis, the University of Newcastle Australia.

Pineda, J.A., Romero, E., Alonso, E.E. and Perez, T. 2014a. "A new high-pressure triaxial apparatus for inducing and tracking hydro-mechanical degradation of clayey rocks." Geotechnical Testing Journal, 37(6), 933-947. http://dx.doi.org/10.1520/GTJ 2013013

Pineda, J.A., Alonso, E.E. and Romero, E. 2014b. "Environmental degradation of claystones." Geotechnique, 64(1), 64-82. https://doi.org/10.1680/geot.13.P.056

Romero, E.E., Garcia, I. and Knobelsdorf, J. 2005. "Gas permeability evolution of a sand/bentonite during controlled-suction paths." Proceedings of the International Symposium on Advanced Experimental Unsaturated Soil Mechanics, 385-390. https://doi.org/10.1016/j.enggeo.2022.106966

Romero, E., Senger, R., Marschall, P. and Gómez, R. 2012. "Air tests on low-permeability claystone formations. Experimental results and simulations." In Multiphysical testing of soils and shales (eds L. Laloui and A. Ferrari), 69–83, https://doi.org/10.1007/978-3-642-32492-5_6

William, E. and Airey, D. 2004. "Index properties and the engineering behaviour of Bringelly shale." Australian Geomechanics Journal, 39(3), 31-42.

Yoshimi, Y. and Osterberg, J.O. 1963. "Compression of partially saturated cohesive soils." Journal of the Soil Mechanics and Foundations Division, ASCE, 89, 1-24. https://doi.org/10.1061/JSFEAQ.0000523